This research was funded in whole or in part by National Science Centre, Poland 2020/39/O/ST7/02897.

A Circular Waveguide Dual-Mode Filter with Improved Out-of-Band Performance for Satellite Communication Systems

Michal Baranowski, *Graduate Student Member, IEEE*, Łukasz Balewski, Adam Lamecki, *Senior Member, IEEE*, Michal Mrozowski, *Fellow, IEEE* and Jaione Galdeano

***Abstract*—This letter presents a novel design for a 3D-printed circular waveguide dual-mode (CWDM) filter with a modified cavity shape. The modification leads to a wide spurious-free stopband, which is highly desirable for channel separation in waveguide contiguous output multiplexers (OMUXs) in satellite communication systems. The new resonant cavity design is a result of applying shape deformation to a basic circular cavity in order to move away and suppress parasitic modes. A fourth-order Ku-band channel filter with two transmission zeros is designed, fabricated by additive manufacturing (AM) in one piece and measured. In comparison with the state-of-the-art design of a stepped CWDM filter, an improvement of approximately 35% wider spurious-free range is achieved.**

***Index Terms*—dual-mode waveguide filters, output multiplexer (OMUX), shape deformation, additive manufacturing.**

I. Introduction

In modern satellite communication systems, there is an ongoing need to increase the capacity of the provided services. To meet this demand, a larger number of transponders need to be allocated, which raises the requirements for satellite payload systems. This mostly concerns the design of contiguous channel output multiplexers (OMUXs) [1], [2], which are among the most specialized microwave passive components comprising the satellite payload. The key requirement for OMUX systems is to accommodate multiple channels and exhibit a high power-handling capability and low transmission losses. Therefore, channel filters for OMUX applications should be narrowband, highly selective, as well as maintain a high Q-factor and high power handling. For this reason, the most preferred choice for an OMUX channel filter is the circular waveguide dual-mode (CWDM) cavity filter [3], [4], which has been subject to many modifications and improvements over the years [5]–[7]. This filter type typically operates with TE_{11n} modes, n = 1–4, which offer high Q-factors, and the dual-mode cavity arrangement allows the realization of advanced filter response with transmission zeros (TZs). However, the conventional CWDM filter has a poor out-of-band performance, which is a major limiting factor in the design of OMUXs with many channels and wide working bandwidths.

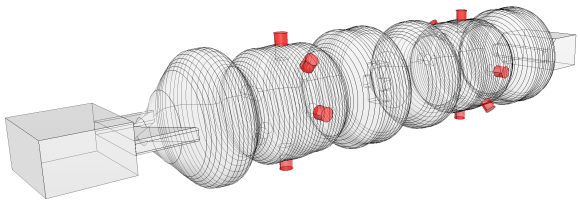

Fig. 1. Geometry of the proposed deformed circular waveguide dual-mode filter.

In order to accommodate more channels in a single multiplexer manifold and eliminate additional lowpass filters from the OMUX, one of the most critical challenges is to design channel filters which do not interfere with each other and thus have a stopband covering the entire operating bandwidth. The most efficient design to date improving the spurious mode separation is the stepped CWDM filter [8], which can provide an approximately 35% wider spurious-free window than the conventional CWDM design. For Ku-band OMUX realizations, this solution covers the spurious-free region from 10.5 up to 12 GHz, enabling the realization of a 17-channel OMUX with a 1 GHz included bandwidth (10.7–11.72 GHz). However, this is still a relatively narrow spurious-free band and it will be shown that further improvements can be made in this area.

In this letter, a new Ku-band channel filter incorporating a deformed circular waveguide dual-mode cavity operating with quasi-TE_{113} mode is presented. The proposed solution, presented in Figure 1, offers a wide spurious-free band ranging from 10.6 to 12.7 GHz, which would allow the realization of a wideband OMUX (up to 2 GHz included bandwidth). A prototype fourth-order filter with two TZs was fabricated using selective laser melting (SLM) 3D printing technology and measured to verify this design.

Manuscript received May 30, 2022; revised July 1, 2022; accepted July 22, 2022. Date of publication ..., 2022; date of current version ..., 2022.

M. Baranowski, A. Lamecki, and M. Mrozowski are with the Faculty of Electronics, Telecommunications, and Informatics, Gdańsk University of Technology, 80-233 Gdańsk, Poland (e-mail: m.baranowski@ieee.org; adam.lamecki@ieee.org; m.mrozowski@ieee.org).

Ł. Balewski and A. Lamecki are with EM Invent Sp. z o.o. (limited company), Trzy Lipy 3, 80-172 Gdańsk, Poland (e-mail: lukasz.balewski@eminvent.com).

J. Galdeano is with the European Space Research and Technology Center, European Space Agency, 2201 AZ Noordwijk, The Netherlands (e-mail: jaione.galdeano@esa.int).

This work was supported by the National Science Centre, Poland under agreement 2020/39/O/ST7/02897 and the European Space Agency under contract 4000128097/19/NL/CBi.

II. Resonant Cavity Analysis

The basis for this work is a conventional circular waveguide cavity operating with two orthogonal TE_{113} modes. This classic CWDM cavity was closely examined in terms of Q-factor and spurious mode separation. Then, various cavity shape modifications were investigated to achieve an improvement in the spurious-free region over the state-of-the-art stepped CWDM cavity [8], while maintaining a similar unloaded Q. The edges of the basic cylindrical cavity were filleted to form a smooth "pill" shape, which was then modified using shape deformation with radial basis functions [9]. The basic principle of this technique is to define a set of points around the object that will control the deforming operation. The deformation is performed by shifting some of these control points to certain new coordinates, and the original structure is then smoothly reshaped according to this displacement. The starting point in this investigation was to squeeze the "pill" cavity shape at two longitudinal positions: at one third and at two thirds of the cavity length, maintaining axial symmetry. Such deformation suppresses the spurious mode—in this case, the TE_{211} mode—while having little effect on the operating TE_{113} mode. This can be observed in the mode chart provided in Figure 2.

Next, the shape deformation technique was coupled with an eigenmode solver from the 3D finite-element method (FEM) electromagnetic (EM) field simulator InventSim [10], with aim of finding an optimal cavity shape for Q and higher-order mode separation. The design procedure involved managing the geometrical parameters of the basic structure (cylinder length and radius) and the shape deformation parameters (deformation location and depth). Conventional, stepped, and deformed CWDM cavities are compared in Table I. It can be observed that the deformed cavity provides an over 50% wider spurious-free band than the stopped CWDM cavity, with only a minor decrease in unloaded Q. The cavity was then modified to be compliant with the restrictions of 3D printing—that is, to ensure the structure is not tilted at an angle greater than $45°$ along the printing axis (the cavity axis). Both modified cavities are shown in Figure 3. The 3D-printable cavity is also included for comparison in Table I. Adjustment of the prepared cavity resulted in a slight deterioration of its Q-factor and out-of-band performance, but nonetheless the final structure yields a significant improvement in terms of spurious mode suppression over the state-of-the-art solutions.

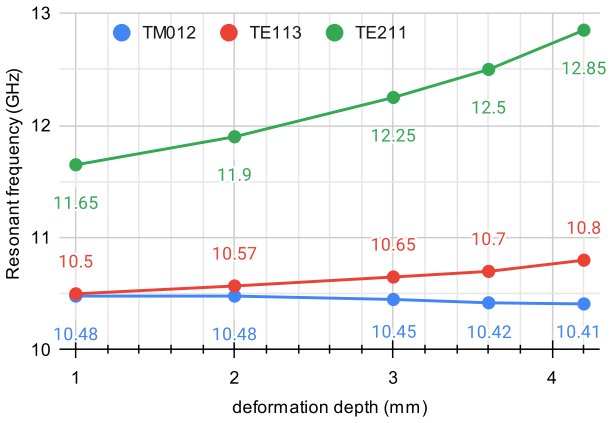

Fig. 2. The mode chart of a deformed CWDM cavity illustrating the effect of cavity deformation on the operating and adjacent modes.

TABLE I
Analysis of Cylindrical Cavity Resonators

cavity type	conventional CWDM	stepped CWDM [8]	deformed CWDM	modified def. CWDM*
f_{TE113} (GHz)	10.85	10.73	10.85	10.9
f_{lower} (GHz)	10.6	10.5	10.58	10.5
f_{higher} (GHz)	11.8	12.0	12.96	12.77
Q_u (silver)	20700	19100	18000	17800
spurious-free region (GHz)	1.2	1.5	2.38	2.27
upper stopband	$1.09f_0$	$1.12f_0$	$1.19f_0$	$1.17f_0$

* the deformed CWDM cavity was modified (cut $45°$) to allow it to be 3D-printed in a single piece.

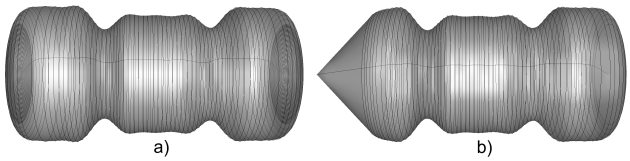

Fig. 3. Geometry of the proposed deformed CWDM cavity: a) optimal shape, b) prepared for 3D printing.

III. Filter Design and Fabrication

A. Filter Design

The new dual-mode cavities were then used to design a fourth-order Ku-band channel filter with two TZs. This filter has been designed for the lowest-frequency channel of a wideband OMUX with an operating bandwidth of 10.7–12.7 GHz. The design specifications are: center frequency $f_0 = 10.8$ GHz, bandwidth BW = 72 MHz and a return loss RL $>$ 21 dB. The two TZs are centered at 10.73 GHz and 10.87 GHz. The synthesized coupling matrix of the filter prototype is given in Table II. The new filter design is composed of the two deformed CWDM cavities, coupled via a cross iris and interfaced at input and output with a WR-75 waveguide standard, as shown in Figure 1. The design is tuned by a total of twelve standard M3 tuning screws, with six screws for each dual-mode cavity. The design was optimized by altering the tuning screws and the widths and heights of the coupling irises. The zero-pole method was used as the optimization technique [11], [12]; this is available as a module in the InventSim EM field simulator.

B. Fabrication and Measurement

A prototype of the new filter was manufactured in one piece using the SLM process [13], [14] using a TruPrint 2000 printer

TABLE II
Coupling Matrix Coefficients

MS1 = 1.045	M14 = -0.196	M34 = 0.887
M12 = 0.887	M23 = 0.788	M4L = 1.045

This article has been accepted for publication in IEEE Microwave and Wireless Components Letters. This is the author's version which has not been fully edited and content may change prior to final publication. Citation information: DOI 10.1109/LMWC.2022.3193722

from Trumpf with an aluminum-silicon-based alloy AlSi10Mg. It should be noted that the conductivity and surface roughness obtained in the process significantly limit the Q-factor of the filter. The prototype was tuned using silver-plated M3 screws. The measurement setup, which employs a vector network analyzer (VNA), is visible in Figure 4a.

A comparison of the simulation and measurement results is given in Figure 4. The measured passband response, shown in Figure 4a, is in excellent agreement with the simulation. The bandwidth is 2 MHz narrower than expected, but the filter otherwise matches the specifications. The in-band insertion loss at f_0 is IL = 1.03 dB and the return loss is greater than 21 dB. Based on the measured IL, the extracted Q of the filter is 2500, which corresponds to an effective conductivity of $\sigma_{eff} = 1.72 \cdot 10^6$ S/m. This value is comparable to other reported aluminum structures fabricated with SLM [9], [15], [16]. This estimated conductivity σ_{eff} was taken into account in the EM simulations shown in this comparison. The measured wideband response is provided in Figure 4b. The fabricated filter guarantees a very wide upper spurious-free stopband up to 12.7 GHz (1.17 f_0).

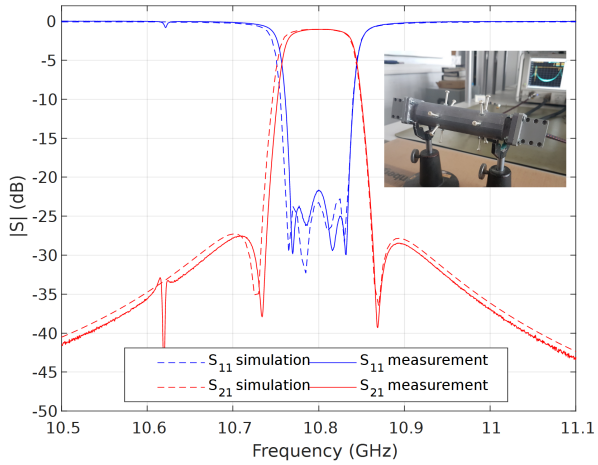

(a)

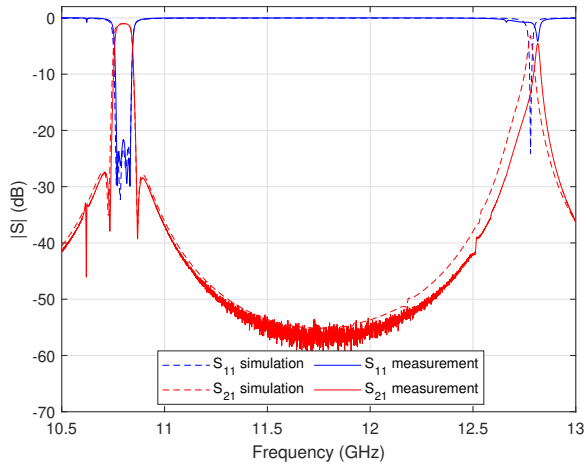

(b)

Fig. 4. Comparison of simulations and measurement for the proposed dual-mode filter. (a) passband response. (b) wideband response.

TABLE III
COMPARISON WITH STATE-OF-THE-ART OMUX CHANNEL FILTERS

Ref.	this work	CWDM	[8]	[17]	[18]	[19]
f_0 (GHz)	10.8	10.73	10.73	11.52	20.175	11.483
FBW (%)	0.67	0.5	0.5	0.32	0.16	0.47
Order	4	4	4	5	4	4
No. of TZs	2	2	2	2	2	2
Q	2500 / 14500*	14000 (Al)	12800 (Al)	15500 (Ag)	25500 (Ag)	2900 / 12500*
IL	1.0 / 0.2*	0.2	0.25	0.45	0.4	1.0 / 0.8*
spurious-free region (GHz)	10.6–12.7	10.6–11.7	10.5–12	9.3–12.5	19.5–20.9	8.2–12.4
upper stopband	$1.17f_0$	$1.09f_0$	$1.12f_0$	$1.09f_0$	$1.04f_0$	$1.08f_0$
cavity type	deformed CWDM	CWDM	stepped CWDM	dielectric-loaded	super Q DM	spherical DM

* Q or IL of the measured 3D-printed prototype vs. simulation result for silver.

C. Comparison and Discussion

A comparison of the proposed deformed CWDM filter with other channel filters for OMUX applications [8], [17]–[19] is presented in Table III. It can be concluded, of the state-of-the-art solutions included in this comparison, the one presented in this letter offers the widest upper stopband clear of spurious modes. This is an improvement in terms of its spurious-free range, which is about 35% greater than that of the stepped cavity filter and nearly 90% greater than that of a classic CWDM cavity filter. The limited Q of the manufactured filter results from the high surface roughness of the 3D-printed metal, and could be overcome by silver plating the inside walls of the filter. The simulated Q-factor of the silver-plated component is $Q_{Ag} = 14500$, comparable to other reported designs. It should be pointed out that, while the Q-factor achievable with the SLM process we used for fabricating the filter prototype is much lower than for the silver plated filters machined with CNC, a state-of-the-art SLM using a proprietary process was recently reported [20], and involves postprocessing of the surfaces by depositing copper and then silver plating, resulting in an efficient conductivity of $2.5 \cdot 10^7$ S/m, which is an order of magnitude greater than what we could achieve. Consequently, with appropriate postprocessing, SLM can become competitive with traditional fabrication processes for filter applications, including in terms of insertion loss.

IV. CONCLUSION

In this letter we report on a new Ku-band channel filter employing a deformed circular waveguide dual-mode cavity shape. The new cavity design is achieved by applying shape deformation to a conventional cylindrical cavity in order to achieve a better out-of-band performance. A highly selective narrowband fourth-order filter was designed and manufactured using AM technology. The fabricated filter demonstrates a very wide upper stopband, which would allow realization of a wideband manifold-coupled OMUX without the insertion of any additional lowpass filters.

REFERENCES

[1] C. Kudsia, R. Cameron, and W.-C. Tang, "Innovations in microwave filters and multiplexing networks for communications satellite systems," *IEEE Trans. Microw. Theory Techn.*, vol. 40, no. 6, pp. 1133–1149, June 1992.

[2] R. I. Cameron and M. Yu, "Design of manifold-coupled multiplexers," *IEEE Microw. Mag.*, vol. 8, no. 5, pp. 46–59, Oct. 2007.

[3] A. Williams, "A four-cavity elliptic waveguide filter," *IEEE Trans. Microw. Theory Techn.*, vol. 18, no. 12, pp. 1109–1114, Dec. 1970.

[4] A. Atia and A. Williams, "Narrow-bandpass waveguide filters," *IEEE Trans. Microw. Theory Techn.*, vol. 20, no. 4, pp. 258–265, April 1972.

[5] M. Guglielmi, R. Molina, and A. Melcon, "Dual-mode circular waveguide filters without tuning screws," *IEEE Microw. Guided Wave Lett.*, vol. 2, no. 11, pp. 457–458, Nov. 1992.

[6] L. Accatino, G. Bertin, and M. Mongiardo, "Elliptical cavity resonators for dual-mode narrow-band filters," *IEEE Trans. Microw. Theory Techn.*, vol. 45, no. 12, pp. 2393–2401, Dec. 1997.

[7] K.-L. Wu, "An optimal circular-waveguide dual-mode filter without tuning screws," *IEEE Trans. Microw. Theory Techn.*, vol. 47, no. 3, pp. 271–276, Mar. 1999.

[8] H. Hu, K.-L. Wu, and R. J. Cameron, "Stepped circular waveguide dual-mode filters for broadband contiguous multiplexers," *IEEE Trans. Microw. Theory Techn.*, vol. 61, no. 1, pp. 139–145, Jan. 2013.

[9] M. Baranowski, L. Balewski, A. Lamecki, M. Mrozowski, and J. Galdeano, "The design of cavity resonators and microwave filters applying shape deformation techniques," *TechRxiv (preprint)*, Feb. 2022.

[10] *InventSim*. (2022). EM Invent. [Online]. Available: http://inventsim.com/.

[11] P. Kozakowski and M. Mrozowski, "Automated CAD of coupled resonator filters," *IEEE Microw. Wireless Compon. Lett.*, vol. 12, no. 12, pp. 470–472, Dec. 2002.

[12] L. Balewski, G. Fotyga, M. Mrozowski, M. Mul, P. Sypek, D. Szypulski, and A. Lamecki, "Step on it!: Bringing fullwave finite-element microwave filter design up to speed," *IEEE Microw. Mag.*, vol. 21, no. 3, pp. 34–49, Mar. 2020.

[13] F. Calignano, D. Manfredi, E. P. Ambrosio, S. Biamino, M. Lombardi, E. Atzeni, A. Salmi, P. Minetola, L. Iuliano, and P. Fino, "Overview on additive manufacturing technologies," *Proc. IEEE*, vol. 105, no. 4, pp. 593–612, April 2017.

[14] O. A. Peverini, M. Lumia, F. Calignano, G. Addamo, M. Lorusso, E. P. Ambrosio, D. Manfredi, and G. Virone, "Selective laser melting manufacturing of microwave waveguide devices," *Proc. IEEE*, vol. 105, no. 4, pp. 620–631, April 2017.

[15] M. D. Benge, R. C. Huck, and H. H. Sigmarsson, "X-band performance of three-dimensional, selectively laser sintered waveguides," in *Proc. IEEE Antennas Propag. Soc. Int. Symp. (APS/URSI)*, July 2014, pp. 13–14.

[16] F. Zhang, C. Guo, Y. Zhang, Y. Gao, B. Liu, M. Shu, Y. Wang, Y. Dong, M. J. Lancaster, and J. Xu, "A 3-D printed bandpass filter using TM_{211}-mode slotted spherical resonators with enhanced spurious suppression," *IEEE Access*, vol. 8, pp. 213 215–213 223, 2020.

[17] A. Panariello, M. Yu, and C. Ernst, "Ku-band high power dielectric resonator filters," *IEEE Trans. Microw. Theory Techn.*, vol. 61, no. 1, pp. 382–392, Jan. 2013.

[18] B. Yassini and M. Yu, "Ka-band dual-mode super Q filters and multiplexers," *IEEE Trans. Microw. Theory Techn.*, vol. 63, no. 10, pp. 3391–3397, Oct. 2015.

[19] L. Qian, Y. Wang, S. Li, A. E.-M. A. Mohamed, M. M. Attallah, T. Skaik, P. Booth, L. Pambaguian, C. M. España, and P. Martín-Iglesias, "A narrowband 3-D printed invar spherical dual-mode filter with high thermal stability for OMUXs," *IEEE Trans. Microw. Theory Techn.*, vol. 70, no. 4, pp. 2165–2173, April 2022.

[20] S. Sirci, E. Menargues, and M. Billod, "Space-qualified additive manufacturing and its application to active antenna harmonic filters," in *2021 IEEE MTT-S Int. Microw. Filter Workshop (IMFW)*, 2021, pp. 239–242.